Cyclotron Resonance Feature in the X-ray Spectrum and Pulse Period Variations of GX 304−1 during the Outbursts in 2010 with MAXI/GSC, Suzaku, and RXTE

Takayuki Yamamoto,[12]
Tatehiro Mihara,[2] Motoki Nakajima,[3] Mutsumi Sugizaki[2] Kazutaka Yamaoka[4] and Masaru Matsuoka[2]

[1] Department of Physics, Nihon University, 1-8-14 Surugadai, Chiyoda, Tokyo 101-8308, Japan
[2] MAXI team, RIKEN, 2-1 Hirosawa, Wako, Saitama 351-0198, Japan
[3] School of Dentistry at Matsudo, Nihon University, 2-870-1 Sakaecho-nishi, Matsudo, Chiba 101-8308, Japan
[4] Department of Physics and Mathematics, Aoyama Gakuin University, 5-10-1 Fuchinobe, Chuo, Sagamihara, Kanagawa 252-5258, Japan
E-mail(TY): tyamamot@crab.riken.go.jp

Abstract

MAXI/GSC has detected outbursts from GX 304−1 four times every 132.5-day interval during the first one-year operation since August 2009. The third outburst in August 2010 reached a flux of 600 mCrab in a 2–20 keV band, which is the highest ever observed from this source. We conducted the follow-up observation by Suzaku and RXTE, then discovered the cyclotron resonance feature (CRSF) at around 54 keV, which is the first CRSF detection from this source. The estimated strength of surface magnetic field, 4.7×10^{12} G, is one of the highest among binary X-ray pulsars from which CRSFs have ever been detected.

Key words: stars: magnetic fields — pulsars: individual (GX 304−1) — stars: neutron — X-rays: binaries

1. Introduction

The magnetic field strength of neutron stars is one of the important parameters related to their fundamental physics. The surface magnetic field of accreting X-ray pulsars can be best estimated from the Cyclotron Resonance Scattering Feature (CRSF) in their X-ray spectra. The CRSFs have ever been detected from 15 X-ray pulsars, and their surface magnetic fields are found to be distributed within a relatively narrow range of $(1-4) \times 10^{12}$ G (e.g. Trumper et al. 1978; White et al. 1983; Mihara 1995; Makishima et al. 1999; Coburn et al. 2002; and references therein).

Since 1980, GX 304−1 had been in an X-ray off state (Pietsch et al. 1986) and no significant X-ray emission was detected for 28 years. Its quiescence was broken by the hard X-ray detection with INTEGRAL in 2008 June (Manousakis et al. 2008). Since then, the source seemed to return to the active state. Actually, from November 2009 to January 2011, MAXI and Swift have detected three outbursts every 132.5-day interval (Yamamoto et al. 2009; Krimm et al. 2010; Mihara et al. 2010a).

We here report the discovery of a CRSF in RXTE and Suzaku X-ray spectra of GX 304−1, obtained during the outbursts in August 2010 through follow-up observations triggered by MAXI. We also discuss a possible change of the observed CRSF energy related to the X-ray flux.

2. Observations

2.1. MAXI

MAXI/GSC (Matsuoka et al. 2009, Mihara et al. 2011) has been monitoring the flux of GX 304−1 since the mission start (Sugizaki et al. 2011). Figure 1 shows the MAXI/GSC light curve of GX 304−1 from 2009 August 15 (MJD=55058) to 2011 January 31 (MJD=55592). Four outbursts were detected with an interval of 132.5-day, which is consistent with the orbital period suggested from the Vela 5B data (Priedhorsky and Terreletl 1983). The peak intensities of the first three outbursts gradually increased. In the 2–20 keV band, the outburst in 2010 August reached 0.6 Crab, which is the highest among flaring events ever observed from this source.

2.2. Suzaku

A Suzaku ToO observation of GX 304−1 was performed on 2010 August 13, two days before the outburst maximum. It was triggered by the MAXI detection of the rapid flux increase (Mihara et al. 2010a). The Suzaku data covers an energy band from 0.5 to 500 keV, using

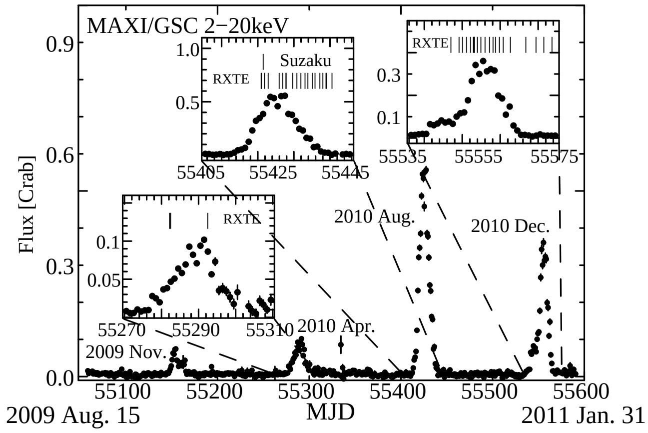

Fig. 1. MAXI/GSC light curve of GX 304−1 in 2–20 keV band from 2009 August 15 to 2011 January 31. The left, center and right inset shows a zoom up around the outburst from 2010 March 15 to April 24, 2010 July 28 to September 6 and 2010 December 5 to 2011 January 14, respectivery. The RXTE and Suzaku observations are indicated with bars in each inset.

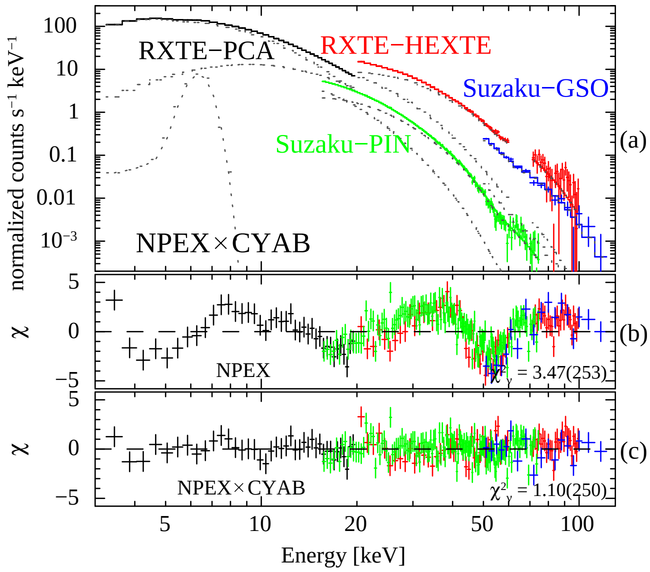

Fig. 2. X-ray spectra of GX 304−1 observed by RXTE and Suzaku on August 13-14. (a) Data and best fit spectral models of NPEX×CYAB. (b) Residuals of best-fit NPEX model. (c) Residuals of best-fit NPEX with a single CYAB model.

the X-ray Imaging Spectrometer (XIS: Koyama et al. 2007) and the Hard X-ray Detector (HXD: Takahashi et al . 2007, Kokubun et al. 2007). The target was placed at the HXD nominal position on the detectors. The XIS was operated in the normal mode with 1/4-window and 0.5 s burst options, which gives a time resolution of 2 s. The HXD was operated in the nominal mode.

2.3. RXTE

RXTE ToO (Target of Opportunity) observations of GX 304−1 were performed during the outbursts in 2010 March, August and December, and gave useful data in the energy range from 3 to 250 keV with the Proportional Counter Array (PCA: Jahoda et al. 2006) and the High-Energy X-ray Timing Experiment (HEXTE: Rothschild et al. 1998). The total 44 observations were carried out, with exposure of 0.5–10 ks each. The observation epochs are indicated in figure 1.

3. Analysis and Results

3.1. Spectral Analysis

The RXTE and Suzaku observations both provide us with an opportunity to search for CRSFs that have not been detected from GX 304−1 in the X-ray energy band up to 40 keV (White et al. 1983). Hereafter we concentrate on the analysis of pulse-phase-averaged spectra for CRSFs.

We present results using the data of the PCA (3–20 keV) and the HEXTE (20–100 keV) from RXTE, and those of HXD-PIN (15–75 keV) and HXD-GSO (50–130 keV) from Suzaku. The Suzaku XIS data were not used in the spectral analysis, because they suffer some event pile-up.

3.1.1. CRSF in X-ray Spectra by RXTE and Suzaku

We first performed joint spectral fits to the data taken by RXTE and Suzaku during 12 hours from August 13 16:00 (UT), as presented in figure 2. Since these observations are not exactly simultaneous, the average flux can be different between the two data sets. We thus introduced a parameter representing relative normalization of the over all model, and allowed it to take defferent values among the PCA, HEXTE, HXD-PIN, and HXD-GSO spectra. The four values of this parameter agreed with one another within calibration uncertainties.

We here examined the validity of the RXTE-HEXTE background spectrum. The energy band from 61 keV to 71 keV was ignored in all the subsequent analysis since artificial structures are known to remain for the data taken after 2009 December.

We employed an NPEX (Negative and Positive power laws with exponential cutoff: Mihara 1995; Makishima et al. 1999) model to reproduce the continuum from 3 keV to 130 keV. In the NPEX model we left free all parameters but one : the positive power-law index, α_2, was fixed at 2.0, representing a Wien peak, because it was not well constrained by the data. The fit with either NPEX alone was unacceptable ($\chi^2_\nu = 3.47$ for $\nu = 253$, respectively). As shown in figure 2 (b), the residuals exhibit absorption features around 40–60 keV in both the RXTE and the Suzaku spectra.

We then multiplied the continum models with cyclotron absorption (CYAB) factors (Mihara et al. 1990;

Table 1. Summary of joint fits to Suzaku and RXTE spectra taken on 2010 August 13-14

Parameter	Model	
	NPEX	NPEX×CYAB
N_{H} (10^{22} cm^{-2})	4.22	$3.13^{+0.24}_{-0.26}$
$I_{\mathrm{Fe}}{}^{a}$ ($\times10^{-2}$)	0.81	$0.91^{+0.13}_{-0.13}$
$A_1{}^{b}$ ($\times10^{0}$)	0.92	$0.72^{+0.03}_{-0.03}$
α_1	0.57	$0.49^{+0.02}_{-0.02}$
kT (keV)	6.5	$7.4^{+0.2}_{-0.2}$
$A_2{}^{b}$ ($\times10^{-4}$)	9.4	$5.2^{+0.5}_{-0.6}$
E_{a1} (keV)	—	$53.7^{+0.7}_{-0.6}$
W_1 (keV)	—	$10.2^{+2.3}_{-2.0}$
D_1	—	$0.73^{+0.09}_{-0.06}$
χ^2_ν (ν)	3.47 (253)	1.10 (250)

All errors represent the 90% confidence limits of the statistical uncertainties.
[a] units in photons s^{-1} cm^{-2}.
[b] units in photons s^{-1} cm^{-2} keV^{-1} at 1 keV.

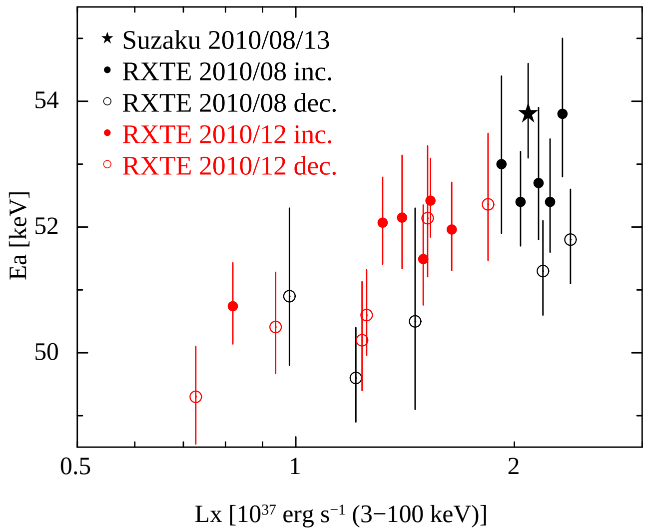

Fig. 3. Relation between the CRSF energy and the 3-100 keV X-ray luminosity during the 2010 August and December outburst. Data points obtained from the RXTE observations of increasing and decreasing phases, and the Suzaku observation are marked with filled circles, open circles, and a star, respectively. The vertical error bars represent the 90% confidence limits of the statistical uncertainty, obtained from the model fits.

Makishima et al. 1999). The NPEX model with a single CYAB feature was accepted within the 90% confidence limit ($\chi^2_\nu = 1.10$ for $\nu = 250$) as shown in figure 2 (c). The fundamental resonance energy was obtained to be $E_{\mathrm{a}} = 53.7^{+0.7}_{-0.6}$ keV. Table 1 summarizes these fitting results and the best-fit model parameters.

3.1.2. CRSF energy variation

As shown in figure 1, the RXTE observations in 2010 August and December covered the peak-to-descent phase of the outburst on an almost daily basis. The data enable us to investigate spectral variations in this period.

With the same procedure as described in subsection 3.1.1., model fits to individual spectra taken in these RXTE observations and the Suzaku were performed. By artificially changing the HEXTE background by ±5% of the nominal value, we confirmed that the obtained best-fit parameters are not sensitive to the background uncertainty.

These spectral fits with NPEX model revealed that the CYAB feature is required by all the spectra of the selected observations with a significance above 90%.

Figure 3 plots the relation between the CRSF energy and the 3–100 keV luminosity, estimated from the best-fit spectral models. The results shows that the CRSF energy depends positively on the X-ray luminosity.

3.2. Timing Analysis

3.2.1. Suzaku

For the timing analysis, a barycentric correction was applied to the arrival times of the X-ray photons using the aebarycen task of Suzaku FTOOLS. Light curves with a time resolutions of 2 s, 3 s and 8 s were extracted from XIS, HXD-PIN, and HXD-GSO event data respectively. We have searched for pulse period with the HXD-PIN data by the efsearch task of xronos, and obtained the pulse period of the pulsar to be 275.5 ± 0.3 s. Pulse profiles were created for eight different energy bands, as shown in Figure 4, and the phase zero was adjusted to the minimum in the XIS 2-7 keV band. The pulse profile consisted of two main peaks and a sub peak in XIS energy range. The first peak (pulse phase 0.0-0.35) disappeared at energies between 10-50 keV. The second peak (pulse phase 0.35-0.7) remained in 0.5-50 keV, and became broader toward higher energies. The width and depth of the dip between the first and the socond pearks decrease gradually with energy up to ∼10 keV. And becomes indistinguishable in the pulse profile avobe 10 keV, making the hard X-ray pulse profiles smooth and single peaked. The first and the second peaks appear again above 50 keV. This is energy band might be related to the cyclotron resonance energy of 54 keV. Pulse fraction is smaller in higher energies, this is consistent with the HEAO-1 observations from White et al. (1983).

3.2.2. RXTE

As shown in figure 1, the RXTE observations in 2010 August and December covered peak-to-descent phase of the outburst on almost daily basis. The data enable us to investigate pulse period variations in this period. RXTE light curves were extracted from Good Xenon data or

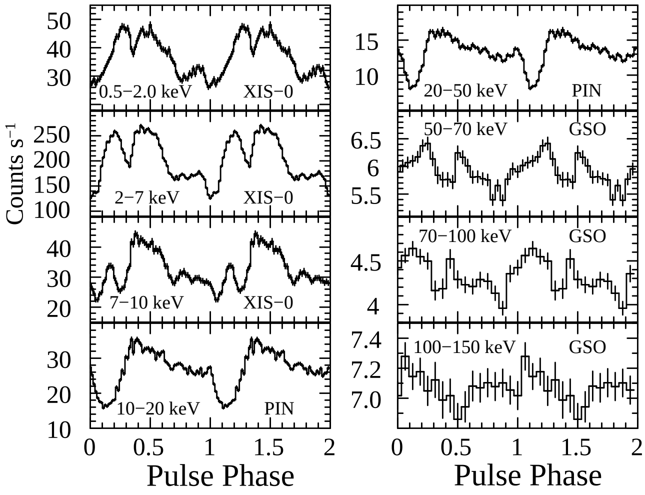

Fig. 4. The Suzaku XIS, HXD-PIN and HXD-GSO pulse profile of GX 304−1 at different energy bands. The error bars represent 1σ uncertainties.

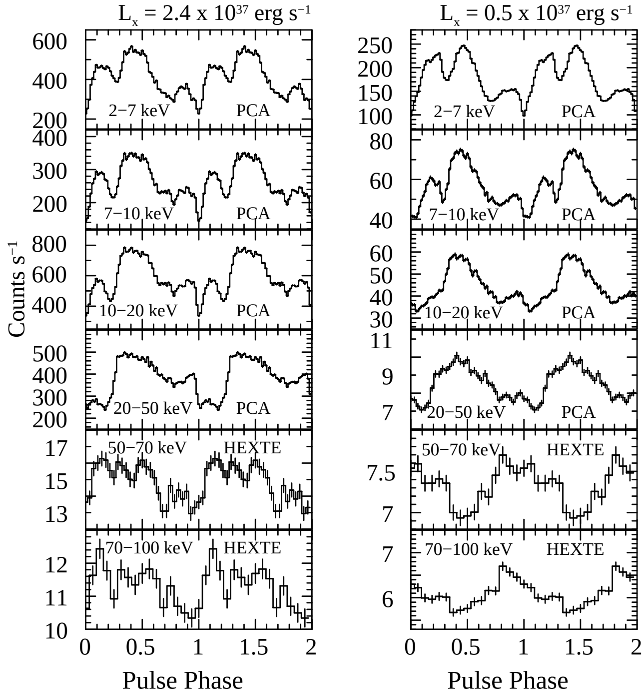

Fig. 5. The RXTE PCA and HEXTE pulse profile of GX 304−1 at different energy bands. The error bars represent 1σ uncertainties. The left and right panel shows a bright and faint phase on outbursts, respectivery.

generic data for PCA, and science data for HEXTE. We performed barycentric correction all PCA and HEXTE light curves. Figure 5 are shown typical pulse profile at bright phase (560 mCrab) and faint phase (150 mCrab). These pulse profiles were almost consistent with the Suzaku observations in soft X-rays, but bothed some difference above 10 keV. In 50-70 keV there are three main peaks in the bright phase while Suzaku had only two. The Suzaku observation was at 400 mCrab, which is between the two phase. In bright phase, first peak still remains in 10-20 keV band. In faint phase, pulse profile were only single peak are scan above 10 keV, and which inverted above 50 keV. We measured pulse period variation of the GX 304−1 during the outburst. We have searched for pulse period, used the adjoin two observation data, to improve the accuracy at the pulse period. Figure 6 show the variations of the pulse period and outbursts light curves. The orbital correction is not applied. The spin-up rate was $\dot{P} = -1.9 \times 10^{-7}$ s s^{-1} in average in 2010 December outburst.

4. Discussion

Since the mission started on 2010 August 15, MAXI detected four X-ray outbursts from GX 304−1 by 132.5-day intervals. As reported by Manousakis et al. 2008, this confirmed the recurrence of the source activities after 28 years of X-ray disappearance. The source may have returned to the active state such that it had been in until 1980. We urge continuous monitoring of this source, and follow-up observations of outbursts with hard X-ray instruments for further studies of the CRSF behaviors.

4.1. Spectroscopy

We analyzed the broadband X-ray (3–130 keV) spectra of GX 304−1 obtained by RXTE and Suzaku, in ToO observations covering the three outbursts in 2010 detected by MAXI. A signature of CRSF was discovered at 54 keV from both the RXTE and the Suzaku data taken on August 13. It is the first detection of the CRSF from this source Mihara et al. (2010b). Sakamoto et al. (2010) reported a Swift-BAT confirmation of the CRSF at around 50 keV from the spectrum accumulating data from August 12 to 17.

The CRSF energy of 54 keV exceeds that of A 0535+26 (∼45 keV: Terada et al. 2006), and becomes the highest among the X-ray binary pulsars whose CRSF parameters are well determined. The surface magnetic field strength is estimated to be 4.7×10^{12} $(1 + z_g)$ G, where z_g represents the gravitational redshift. Makishima et al. 1999 examined the relation between the magnetic field strength estimated from the CRSF and the pulsation period in X-ray binary pulsars, and discussed a group of "slow rotators"; represented by such sources as Vela X-1 and GX 301−2, these objects have much longer pulsation periods than would be expected if they were in rotational equilibria. The obtained field strength of 4.7×10^{12} G, and the pulsation period of 275.47 s measured during the Suzaku observation, place GX 304−1 just in the range of the typical slow rotators.

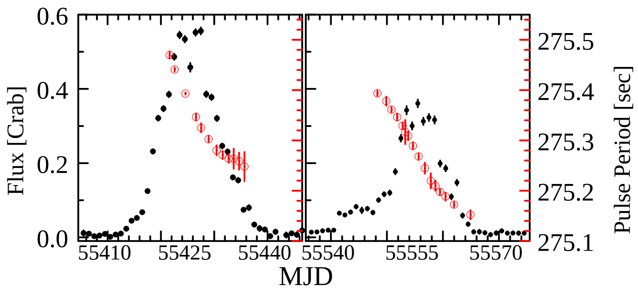

Fig. 6. The light curve and pulse period variation obtained from MAXI/GSC (light curves; black) and RXTE (pulse period; red) observations, the left and right panel shows a 2010 August and December outburst, respectivery. The vertical error bars represent the 1σ uncertainties.

4.2. CRSF energy variation

We performed spectral analysis of the RXTE data covering the outburst in 2010 August and December on an almost daily basis. The CRSF has also been confirmed in 44 RXTE observations in which the source was bright enough. Therefore, the CRSF is persistent in this object. However, the CRSF energy was observed to vary in a positive correlation with the luminosity in $E_{\rm a} \sim 50$ keV to 54 keV.

4.3. Pulse Profiles and Pulse period variation

We detected X-ray pulsations of GX 304−1 as high as above 100 keV, which has not been reported earlier. The pulse profile of GX 304−1 was strongly energy-dependent. It shows a double-peaked profile in the soft X-ray (> 10 keV) and a single peaked smooth profile in hard X-rays as shown in figure 4 and 5. The form double peaked profile at soft X-ray was different from the single-peaked profile in 1.5–10 keV with HEAO−1 (White et al. 1983). Similar energy dependence of pulse profiles are also seen in the Be transient X-ray pulsars A 0535+26 (Caballero et al. 2008), GRO J1008−57 (Naik et al. 2011) and 1A 1118−61 (Devasia et al. 2011). But the recovery of the first peak in the main peak above 50 keV was peculiar to GX 304−1.

Figure 7 show the relation between the pulse period with 3-100 keV luminosity ($PL_{\rm x}^{6/7}$) and the pulse period rate over the pulse period ($\dot{P}/P$). The data is consistent as predictally $PL_{\rm x}^{6/7} \propto -\dot{P}/P$ relations (Longaia et al. 1994).

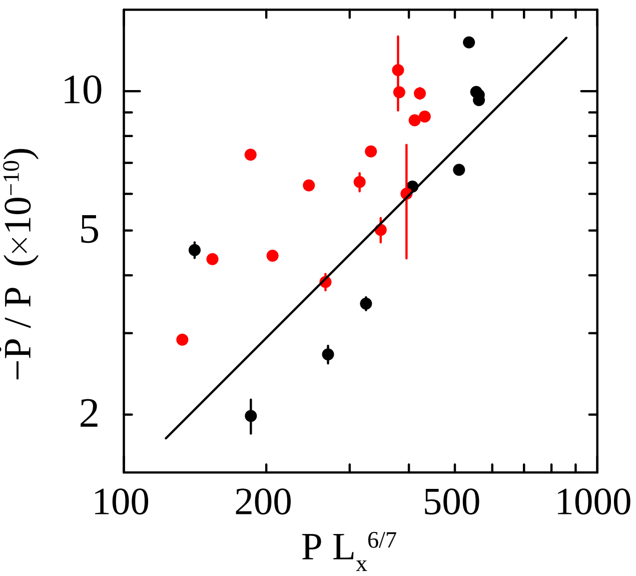

Fig. 7. Relation between the $PL_{\rm x}$ (s (erg s^{-1})$^{6/7}$) and $-\dot{P}/P$ (s^{-1}) during the 2010 August and December outburst. The luminosity $L_{\rm x}$ was erg s^{-1} in 3-100 keV. Data points are from the RXTE observations. The 2010 August and December $PL_{\rm x}^{6/7} \propto -\dot{P}/P$ data are marked with black and red points, respectively. The error bars represent 1σ uncertainties. The line is 1.

References

Yamamoto, T., et al. 2011 PASJ., Suzaku special issue
Caballero, I., et al., 2008, A&A, 480, L17
Coburn, W., et al. 2002, ApJ, 580, 394
Jahoda, K., et al. 2006, ApJS, 163, 401
Devasia, J., et al. 2011, MNRAS,
Kokubun, M., et al. 2007, PASJ, 59, 53
Koyama, K., et al. 2007, PASJ, 59, 23
Krimm, H. A., et al. 2010, ATel #2538
Longaia, M. S., 1994, Cambrige: Cambrige University Press, lc1994, 2nd ed.,
Makishima, K., et al. 1999, ApJ, 525, 978
Manousakis et al., 2008, ATel #1613
Matsuoka, M., et al. 2009, PASJ, 61, 999
Mihara, T., et al. 1990, Nature, 346, 250
Mihara, T., Ph.D. thesis in University of Tokyo 1995
Mihara, T., et al. 2010a, ATel #2779
Mihara, T., et al. 2010b, ATel #2796
Mihara, T., et al. 2011, PASJ, in print.
Naik, S., et al. 2011, MNRAS, 413, 241
Nakajima, M., et al. 2010, ATel #3075
Pietsch, E., et al. 1986, A&A, 163, 93
Priedhorsky, W. C., Terrell, J., 1983, ApJ, 273, 709
Rothschild, R. E., et al. 1998, ApJ, 496, 538
Sakamoto, T., et al. 2010, ATel #2815
Sugizaki, M., et al. 2011, PASJ, Suzaku special issue
Takahashi, T., et al. 2007, PASJ, 59, 35
Terada, T., Mihara, T., Nakajima, M., et al. 2006, ApJ, 648, L139
Trümper, J., et al. 1978, ApJ, 219, L105
White, N., et al. 1983, ApJ, 270, 711
Yamamoto, T., et al. 2009, ATel #2297